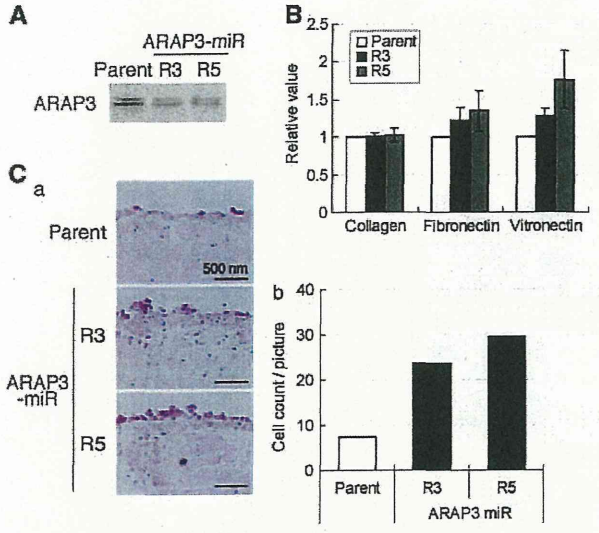

Figure 4 Expression of ARAP3 regulated cell-ECM attachment. ARAP3 was knocked down in 44As3 scirrhous gastric carcinoma cells by a microRNA knockdown system (R3 and R5 cells (**A**)). Cell attachment assays were performed with these cells *in vitro* (**B**) and *ex vivo* (**C**). In the *ex vivo* assay, the attachment of cancer cells to the mesentery was visualized by hematoxylin and eosin staining (C(a)) and quantified by cell counts (C(b)). Knockdown of ARAP3 increased the attachment of gastric carcinoma cells to both the ECM and mesentery.

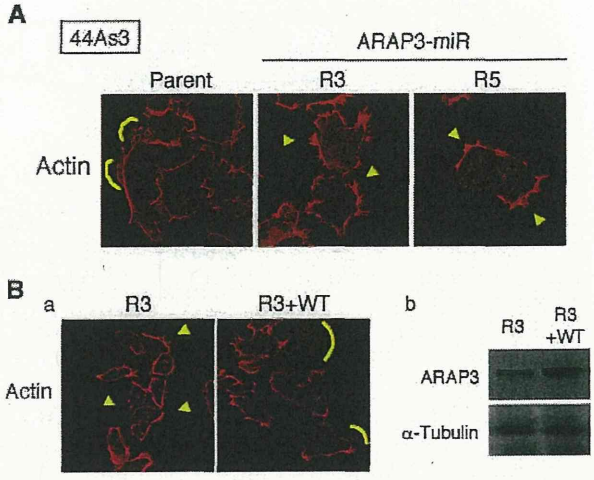

Figure 5 Expression of ARAP3 affected the morphology of the 44As3 cell line. Phalloidin staining for ARAP3 knockdown 44As3 cells (R3 and R5 cells) was performed (**A**). Wild-type ARAP3, which contained silent mutations in the microRNA target sequence, was stably introduced into R3 cells. Morphological changes were shown by phalloidin staining (**B**a) and expression of ARAP3 was detected by western blotting (**B**b). Formation of lamellipodia is indicated with yellow lines and filopodia is marked with yellow arrow heads.

changes (Carragher and Frame, 2004), we examined whether the expression of ARAP3 also affects the cell morphology of the gastric carcinoma cell line. Phalloidin staining showed that R3 and R5 cells formed filopodia instead of the lamellipodia observed in parental 44As3 cells (Figure 5A). Furthermore, introduction of wild-type ARAP3 that contained silent mutations in the target sequence of microRNA into R3 cells suppressed filopodia formation and recovered lamellipodia formation (Figure 5Ba). Expression of mutant ARAP3 was detected with western blotting (Figure 5Bb).

Differential roles of functional domains of ARAP3 in cell adhesion and cell invasion in vitro

As ARAP3 is a multimodular protein (Figure 6A), we investigated the structure–function relationships of ARAP3 domains to peritoneal dissemination. We established three 58As9 cells that expressed mutant ARAP3: (1) an Arf-GAP domain mutant (R532K), (2) a Rho-GAP domain mutant (R942L) and (3) a mutant that lacks both putative tyrosine phosphorylation sites (2YF, Y1403/1408F) (I *et al.*, 2004) (Figure 6A). The level of tyrosine phosphorylation of the ARAP3 2YF mutant was significantly reduced compared with R532K or R942L in 58As9 cells (Figure 6B). As expression levels of ARAP3 were associated with cell morphology in gastric cancer cells (Figure 5), we performed phalloidin staining for 58As9 cells overexpressing ARAP3 mutants. R532K mutant ARAP3 suppressed filopodia formation more strongly than R942L or 2YF mutants (Figure 6C). None of the ARAP3 mutants affected the growth of 58As9 cells (Supplemental Figure 2).

We also studied the effect of overexpression of each mutant ARAP3 on cell-ECM adhesion and invasion. Overexpression of the R532K mutant ARAP3 reduced the attachment of 58As9 cell lines to ECM proteins, but overexpression of the R942L and 2YF mutants did not have any effect (Figure 7A).

As overexpression of wild-type ARAP3 could inhibit the metastasis of 58As9 cells, we performed an *in vitro* migration and invasion assay with the ARAP3 mutant cells. The results of this assay were similar to the attachment assay. Specifically, overexpression of the R532K mutant inhibited cell migration and invasion, but the R942L and 2YF mutants did not have any effect (Figure 7B).

These results suggest that both Rho-GAP function and tyrosine phosphorylation of ARAP3 are necessary to suppress cell-ECM adhesion and invasion of gastric cancer cells. As ARAP3 can inhibit RhoA, which is required for cell invasion (Itoh *et al.*, 1999), we tested whether inhibition of RhoA signal by Y27632, one of the general inhibitors of Rho-associated coiled-coil kinase (ROCK), can also suppress the invasiveness of ARAP3 mutant expressing 58As9 cells. As expected, Y27632 could modestly suppress the invasiveness of the cells (Figure 7Bc).

Functional domains of ARAP3 critical for suppressing peritoneal dissemination in vivo

To investigate whether expression of mutant ARAP3 affects peritoneal dissemination *in vivo*, we injected the

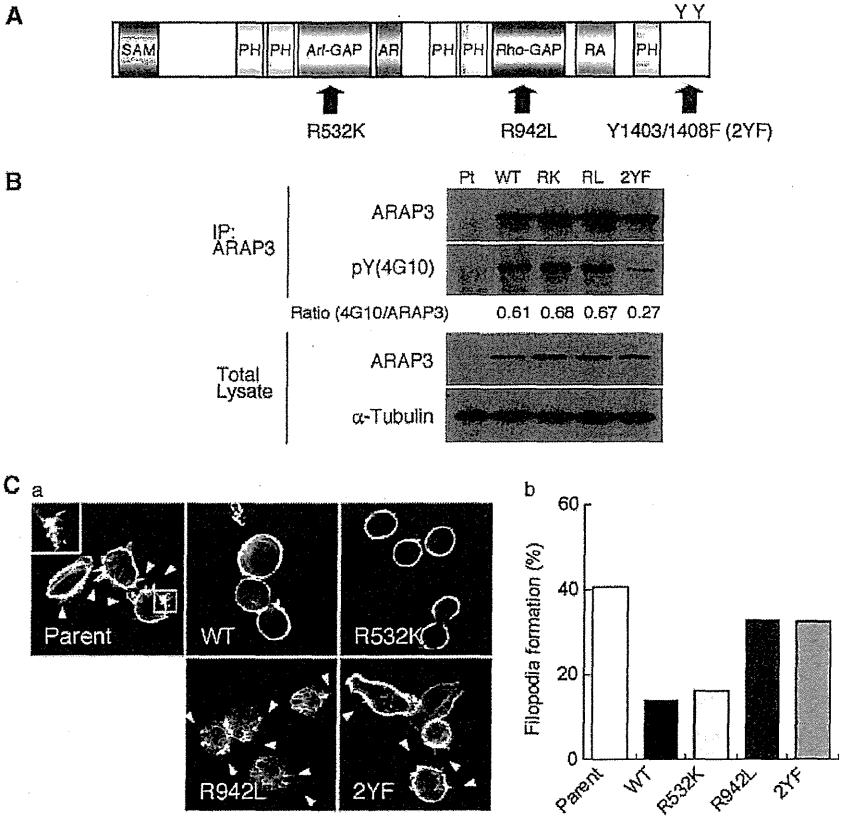

Figure 6 Expression of ARAP3 mutants. Mutations were introduced into the Arf-GAP (R532K) or Rho-GAP (R942L) domain, or into the two putative tyrosine phosphorylation sites (2YF) of ARAP3 (**A**). Expression and tyrosine phosphorylation profiles of 58As9 cells expressing mutant ARAP3 were verified by immunoprecipitation and immunoblotting. The relative tyrosine phosphorylation levels of ARAP3 (phosphorylated ARAP3/total ARAP3) were also calculated (**B**). Morphologies of cells expressing mutant ARAP3 are shown in (**C**). Phalloidin staining was performed on these cells. R532K mutant suppressed the filopodia formation that was observed in the parental cell line, but the R942L and 2YF mutants were not. Filopodia are indicated by white arrows. A highly magnified image of the area that is indicated by the white line is also shown in the image. Quantification of filopodia formation was performed by calculating the percentage of filopodia-positive cells (**C**b). Over 100 cells were counted. SAM, sterile alpha motif; PH, pleckstrin homology domain; AR, ankyrin repeats; RA, Ras association domain (nearly conserved).

cells intraperitoneally into BALB/c nude mice (Figure 8). Parental 58As9 cells showed severe peritoneal dissemination with ascitic fluid as previously described (Yanagihara *et al*., 2005). The R532K mutant suppressed production of ascitic fluid equally effectively, whereas the R942L and 2YF mutants were less effective (Figure 8A). Consistent with this result, expression of R532K, but not R942L and 2YF, suppressed the peritoneal dissemination of 58As9 cells, which was quantified by counting the number of mesentery nodules formed (Figure 8B). These results show that ARAP3 inhibits peritoneal dissemination *in vivo*, and that both the Rho-GAP domain and phosphotyrosine residues at the C-terminus are important for this function.

Discussion

This study showed that ARAP3 is expressed in normal fundic gland mucosa, but its expression is reduced in poorly differentiated carcinomas. ARAP3 inhibited not only cell-ECM attachment and cell invasion *in vitro* but also peritoneal dissemination of 58As9 cells *in vivo*. As adhesion to and invasion through the ECM are essential steps for peritoneal dissemination of scirrhous gastric carcinoma cells, it is hypothesized that ARAP3 suppresses peritoneal dissemination by regulating these processes enhanced in cancer cells.

We first identified ARAP3 while screening for phosphotyrosine proteins in mesentery nodules formed after inoculating nude mice with the 44As3 gastric carcinoma cell line. Unlike other phosphotyrosine proteins identified in this screening, such as FAK, CDCP1 and C9orf10/Ossa, ARAP3 was underexpressed in undifferentiated gastric cancers compared with normal fundic glands. Src pathways are implicated in cancer progression because SFK activity and expression and tyrosine phosphorylation of Src substrates are often elevated in advanced stages of cancer (Yeatman, 2004). Although ARAP3 is a Src substrate, our results showed that tyrosine phosphorylation of ARAP3 conferred

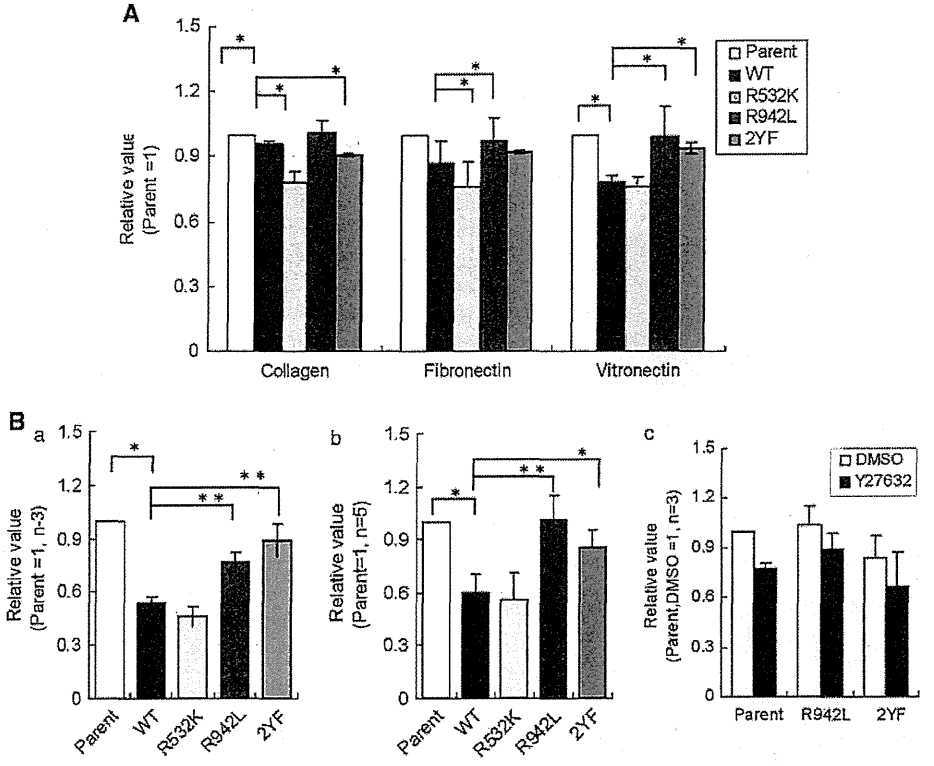

Figure 7 Effects of overexpression of ARAP3 mutants in 58As9 cell lines. Adhesiveness and invasiveness were examined by a cell attachment assay (**A**) and a cell migration and invasion assay (**Ba** and **Bb**, respectively). Overexpressed R942L and 2YF mutants did not rapidly adhere to ECM proteins or suppress cell migration and invasion. The Rho-associated coiled-coil kinase (ROCK) inhibitor Y27632 suppressed the invasiveness of 58As9 cells expressing R942L or 2YF ARAP3 (**Bc**). ARAP3 may suppress the invasiveness of 58As9 cells *in vitro* by inhibiting RhoA activity (*$P<0.05$ **$P< 0.01$).

a tumor suppressive activity. As a result, SFKs may phosphorylate not only oncogenic proteins but also tumor suppressor proteins such as ARAP3.

The ability of ARAP3 to suppress peritoneal dissemination was blocked by a mutation in the Rho-GAP domain, suggesting that this function is mediated by regulation of the Rho family small GTPases. In addition, loss of the C-terminal tyrosine phosphorylation sites of ARAP3 also reduced this suppressive function of ARAP3. However, it is not clear whether Rho-GAP activity and tyrosine phosphorylation of ARAP3 regulate the peritoneal dissemination using an overlapping mechanism or a signal pathway, as no information is available on the phosphotyrosine-mediated signaling of ARAP3. Although we could not detect any change in the activities of Rho family small GTPases in total cell lysate (data not shown), we cannot rule out the possibility that the activation of Rho occurs at the cell surface, because ARAP3 can localize and function there (Krugmann *et al.*, 2002), and its expression actually affected their cytoskeletal reorganization.

Rho family small GTPases are involved in a wide range of cellular processes, such as cell morphology, adhesion and motility. For example, activation of RhoA promotes the stabilization of focal contacts, which are important in the integrin-dependent cell-ECM attachment and cell invasion (Huveneers and Danen, 2009). Filopodia formation is necessary for cell migration and contact sites formation. In neuronal cells, RhoA activity is necessary for the formation of filopodial protrusion induced by RhoA/ROCK signaling (Chen *et al.*, 2006; Kim *et al.*, 2010). Furthermore, activation of mammalian diaphanous-related formin (mDia), which is known as an effector of RhoA, localizes at the filopodia, promotes actin filament assembly and contributes to filopodia formation (Faix and Grosse, 2006; Carramusa *et al.*, 2007; Sarmiento *et al.*, 2008). Therefore, ARAP3 may suppress the cell adhesion, migration and invasion of cancer cells by inhibiting RhoA signaling through its Rho-GAP domain.

ARAP3 is a multimodular protein that can bind to several molecules such as PI(3,4,5)P3 and Src homology 2 domain containing inositol 5-phosphatase 2 (SHIP2) *in vitro*, possibly through its sterile alpha motif domain (Krugmann *et al.*, 2002; Raaijmakers *et al.*, 2007). Our data revealed the essential role of the phosphotyrosine-containing region of ARAP3 for the first time. It might be required to identify molecules that bind to the C-terminal region of ARAP3 in a tyrosine phosphorylation-dependent manner. Further study is needed to determine

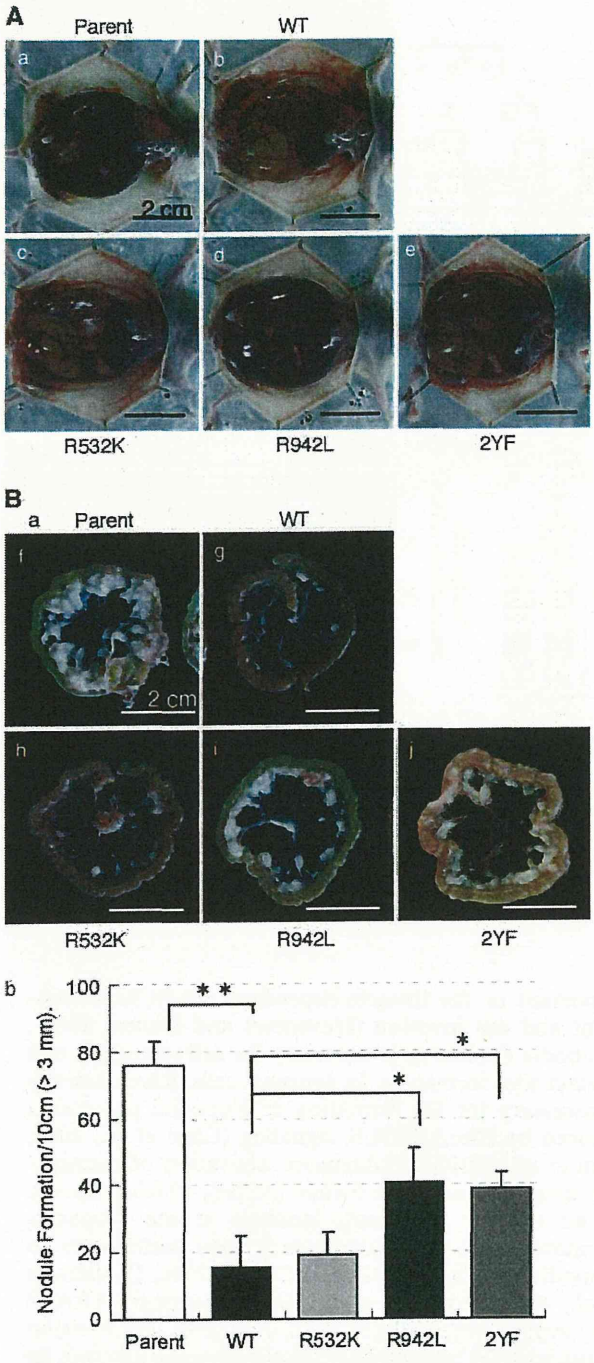

Figure 8 Expression of ARAP3 mutants affects peritoneal dissemination of gastric carcinoma cells. 58As9 cells expressing ARAP3 mutants were injected intraperitoneally into BALB/c nude mice (4×10^6 cells/mouse, $n = 5$). Nineteen days after injection, the R532K mutant ARAP3 suppressed ascites formation and peritoneal dissemination, but the R942L and 2YF mutants did not (**A** and **Ba**). Similarly, R532K also reduced the number of mesentery nodules formed after tumor cell inoculation, whereas R942L and 2YF did not (**Bb**) (*$P<0.05$ **$P<0.01$).

how the phosphotyrosine-dependent signal of ARAP3 suppresses cell-ECM attachment, migration and invasion of cancer cells.

We also observed that the Arf-GAP domain of ARAP3 regulated the internalization of epidermal growth factor receptor following epidermal growth factor stimulation (data not shown), similar to that reported in ARAP1 (Daniele *et al.*, 2008; Yoon *et al.*, 2008). However, judging from the results in this study, the Arf-GAP activity of ARAP3 does not significantly contribute to the suppression of peritoneal dissemination.

Several suppressors of integrin signaling or cell-ECM adhesion have been identified as possible therapeutic targets for preventing peritoneal dissemination of scirrhous gastric carcinoma (Nishimura *et al.*, 1996; Matsuoka *et al.*, 1998). Likewise, ARAP3, which regulates both cell-ECM adhesion and invasiveness, may be a novel therapeutic target. Small molecules that mimic the suppressive function of ARAP3, induce its expression or promote tyrosine phosphorylation of ARAP3 are anticipated to be effective drugs to prevent peritoneal dissemination of scirrhous gastric carcinoma cells.

Materials and methods

Materials

Anti-ARAP3 antibodies used for western blotting were purchased from Abcam (Cambridge, MA, USA), whereas those used for immunohistochemistry were purchased from Santa Cruz Biotechnology (Santa Cruz, CA, USA). Anti-phosphotyrosine (4G10) antibody was obtained from Upstate Biotechnology (Lake Placid, NY, USA). Sheep antimouse antibodies and sheep antirabbit antibodies were bought from GE Healthcare (Buckinghamshire, UK). Rabbit antigoat antibodies were purchased from Zymed (Carlsbad, CA, USA). Alexa 594-conjugated phalloidin was obtained from Molecular Probes (Carlsbad, CA, USA).

Immunohistochemical staining

Paraffin-embedded tissue samples of human scirrhous or non-scirrhous gastric carcinoma were obtained from the National Cancer Center Hospital (Tokyo, Japan). Sections on glass slides were rehydrated and autoclaved at 120 °C for 10 min to reactivate the antigen. Thereafter, the specimens were immunostained using the indirect polymer method with Envision reagent (Dako, Carlsbad, CA, USA) and ARAP3 antibodies (1:500 dilution). Finally, the stained sections were examined with an Olympus BX51 microscope (Tokyo, Japan).

Cell culture

Gastric cancer cell lines (HSC-39, HSC-43, HSC-44PE, 44As3, HSC-58, 58As1, 58As9, HSC-59, HSC-60, HSC-64, KATO3, NKPS, TMK1 and MKN28) were maintained in RPMI 1640 medium (Sigma, St Louis, MO, USA) supplemented with 10% fetal bovine serum (Equitech-Bio, Kerrville, TX, USA) at 37 °C in a humidified atmosphere containing 5% CO_2. G418 (600 ng/ml; Sigma) or Blasticidin (10 ng/ml; Sigma) were also included in the growth medium to select for ARAP3-over-expressing or knockdown cells, respectively.

Construction of ARAP3 Stealth RNAi, miR RNAi and pDONA1-ARAP3 retroviral vectors

The ARAP3 gene was subcloned from a pEGFP-ARAP3 plasmid into a pDON-A1 retrovirus vector, and then mutant

ARAP3 plasmids were constructed using the QuickChange Site-Directed Mutagenesis Kit (Stratagene, Cedar Creek, TX, USA).

The miR RNAi design was based on the sequence of Stealth RNAi, which was designed using the BLOCK-iT RNAi designer tool (https://rnaidesigner.invitrogen.com/rnaiexpress/, Invitrogen, Carlsbad, CA, USA).

Phalloidin staining

Gastric cancer cells cultured on coverslips were fixed with 4% paraformaldehyde for 10 min at room temperature. The samples were incubated with 3% bovine serum albumin for 1 h in Tween-Tris buffered saline (TTBS), followed by incubation with Alexa-594-conjugated phalloidin in TTBS for 45 min at room temperature, and coverslips were mounted on glass slides. The samples were examined using an Olympus IX-70 confocal laser-scanning microscope or an Olympus BX51 microscope for fluorescence microscopy. Phalloidin was used at 1:500 dilutions.

Immunoprecipitation and western blotting

Whole-cell lysates of gastric cancer cells were harvested by PLC lysis buffer (50 mM 4-(2-hydroxyethyl)-1-piperazineethanesulfonic acid (pH 7.5), 150 mM NaCl, 1.5 mM $MgCl_2$, 1 mM ethylene glycol tetraacetic acid, 10% glycerol, 100 mM NaF, 1% Triton X-100, 1 mM sodium orthovanadate, 10 μg/ml leupeptin, 10 μg/ml aprotinin and 1 M phenylmethylsulfonyl fluoride), and used for immunoprecipitation and immunoblotting. Equal amounts of total protein were separated by SDS–polyacrylamide gel electrophoresis and transferred to polyvinylidene fluoride membranes. The membranes were incubated with primary antibodies overnight at 4 °C, and then incubated with Horseradish peroxide (HRP)-conjugated secondary antibodies for 45 min at room temperature. Bands were detected on an X-ray film using an enhanced chemiluminescence system (Perkin elmer, Waltham, MA, USA)). Primary antibodies were used at dilutions of 1:1000 for ARAP3, 1:2000 for α-Tubulin and 1:5000 for phosphotyrosine.

Adhesion test

Cultured gastric cancer cell lines were dissociated with Hank's Balanced Salt Solution containing 0.25 mM EDTA. Cell suspensions (5×10^4 cells/well) were seeded into 24-well plates coated with collagen (Nitta gelatin, Osaka, Japan), fibronectin (Sigma) or vitronectin (TaKaRa, Shiga, Japan) according to the manufacturer's procedure. After incubating the plates for 30 min at 37 °C in a humidified atmosphere containing 5% CO_2, unattached cells were removed by washing with PBS, and then attached cells were trypsinized and counted with a Z1Coulter counter (Beckman Coulter, Brea, CA, USA).

Cell migration and invasion assays

Gastric cancer cells were dissociated with Hank's Balanced Salt Solution containing 0.25 mM EDTA. For the cell invasion assay, cell culture inserts (8.0 μM pore) were coated on the top and bottom surfaces with matrigel (10 μg/well) and fibronectin, respectively. In the cell migration assay, only the bottom surface was coated with fibronectin. Cells (2×10^4) suspended in serum-free RPMI1640 medium were seeded into each cell culture insert. These inserts were then transferred to a culture plate containing RPMI1640 medium with 5% FBS. After incubating at 37 °C in a humidified atmosphere containing 5% CO_2 for 8 h (migration assay) or 12 h (invasion assay), the cells were fixed with 4% paraformaldehyde and stained with Giemsa staining solution. Assays were performed in triplicate.

Ex vivo cell adhesion assay

Ten-millimeter square pieces of the peritoneal wall, including the peritoneum and abdominal skeletal muscle, were excised from 5-week-old BALB/c nude mice. The pieces were placed on top of a layer of 3% agarose gel in culture dishes, with the peritoneum side facing up. Equal numbers of parent 44As3 cells or 44As3 ARAP3 miR cells (4×10^6 cells/dish) were seeded onto the peritoneal tissue, and then incubated in RPMI 1640 medium containing 10% FBS, 50 μg/ml gentamicin, penicillin and streptomycin for 4 weeks. Finally, the cultured peritoneal walls were removed, fixed in 4% paraformaldehyde and embedded in paraffin for histological analysis.

Inoculation of gastric tumor cells into nude mice

Gastric cancer cell lines were trypsinized, and aliquots of 4×10^6 cells were injected intraperitoneally into BALB/c nude mice purchased from CLEA Japan (Tokyo, Japan). After 3 weeks, the mice were killed and dissected. These experiments were approved by the Committee for Ethics of Animal Experimentation and conducted in accordance with the Guidelines for Animal Experiments in the National Cancer Center.

Conflict of interest

The authors declare no conflict of interest.

Acknowledgements

The pEGFP-ARAP3 plasmid was a kind gift from Krugmann S (Cambridge, UK). This work was supported by a Grant-in-Aid for Cancer Research and by a Grant-in-Aid for Scientific Research from the Ministry of Education, Culture, Science and Technology of Japan for the Third Term Comprehensive 10-Year Strategy for Cancer Control.

References

Brown MT, Cooper JA. (1996). Regulation, substrates and functions of src. *Biochem Biophys Acta* **1287**: 121–149.

Carragher NO, Frame MC. (2004). Focal adhesion and actin dynamics: a place where kinases and proteases meet to promote invasion. *Trends Cell Biol* **14**: 241–249.

Carramusa L, Ballestrem C, Zilberman Y, Bershadsky AD. (2007). Mammalian diaphanous-related formin Dia1 controls the organization of E-cadherin-mediated cell-cell junctions. *J Cell Sci* **120**: 3870–3882.

Chen TJ, Gehler S, Shaw AE, Bamburg JR, Letourneau PC. (2006). Cdc42 participates in the regulation of ADF/cofilin and retinal growth cone filopodia by brain derived neurotrophic factor. *J Neurobiol* **66**: 103–114.

Daniele T, Di Tullio G, Santoro M, Turacchio G, De Matteis MA. (2008). ARAP1 regulates EGF receptor trafficking and signalling. *Traffic* **9**: 2221–2235.

Faix J, Grosse R. (2006). Staying in shape with formins. *Dev Cell* **10**: 693–706.

Frame MC. (2002). Src in cancer: deregulation and consequences for cell behaviour. *Biochim Biophys Acta* **1602**: 114–130.

Huveneers S, Danen EH. (2009). Adhesion signaling—crosstalk between integrins, Src and Rho. *J Cell Sci* **122**: 1059–1069.

I ST, Nie Z, Stewart A, Najdovska M, Hall NE, He H *et al.* (2004). ARAP3 is transiently tyrosine phosphorylated in cells attaching to fibronectin and inhibits cell spreading in a RhoGAP-dependent manner. *J Cell Sci* **117**: 6071–6084.

Itoh K, Yoshioka K, Akedo H, Uehata M, Ishizaki T, Narumiya S. (1999). An essential part for Rho-associated kinase in the transcellular invasion of tumor cells. *Nat Med* **5**: 221–225.

Kim HS, Bae CD, Park J. (2010). Glutamate receptor-mediated phosphorylation of ezrin/radixin/moesin proteins is implicated in filopodial protrusion of primary cultured hippocampal neuronal cells. *J Neurochem* **113**: 1565–1576.

Kowanetz K, Husnjak K, Holler D, Kowanetz M, Soubeyran P, Hirsch D *et al.* (2004). CIN85 associates with multiple effectors controlling intracellular trafficking of epidermal growth factor receptors. *Mol Biol Cell* **15**: 3155–3166.

Krugmann S, Anderson KE, Ridley SH, Risso N, McGregor A, Coadwell J *et al.* (2002). Identification of ARAP3, a novel PI3K effector regulating both Arf and Rho GTPases, by selective capture on phosphoinositide affinity matrices. *Mol Cell* **9**: 95–108.

Krugmann S, Andrews S, Stephens L, Hawkins PT. (2006). ARAP3 is essential for formation of lamellipodia after growth factor stimulation. *J Cell Sci* **119**: 425–432.

Krugmann S, Williams R, Stephens L, Hawkins PT. (2004). ARAP3 is a PI3K- and rap-regulated GAP for RhoA. *Curr Biol* **14**: 1380–1384.

Matsuoka T, Hirakawa K, Chung YS, Yashiro M, Nishimura S, Sawada T *et al.* (1998). Adhesion polypeptides are useful for the prevention of peritoneal dissemination of gastric cancer. *Clin Exp Metastasis* **16**: 381–388.

Nishimura S, Chung YS, Yashiro M, Inoue T, Sowa M. (1996). Role of alpha 2 beta 1- and alpha 3 beta 1-integrin in the peritoneal implantation of scirrhous gastric carcinoma. *Br J Cancer* **74**: 1406–1412.

Raaijmakers JH, Deneubourg L, Rehmann H, de Koning J, Zhang Z, Krugmann S *et al.* (2007). The PI3K effector Arap3 interacts with the PI(3,4,5)P3 phosphatase SHIP2 in a SAM domain-dependent manner. *Cell Signal* **19**: 1249–1257.

Sarmiento C, Wang W, Dovas A, Yamaguchi H, Sidani M, El-Sibai M *et al.* (2008). WASP family members and formin proteins coordinate regulation of cell protrusions in carcinoma cells. *J Cell Biol* **180**: 1245–1260.

Tanaka M, Sasaki K, Kamata R, Hoshino Y, Yanagihara K, Sakai R. (2009). A novel RNA-binding protein, Ossa/C9orf10, regulates activity of Src kinases to protect cells from oxidative stress-induced apoptosis. *Mol Cell Biol* **29**: 402–413.

Uekita T, Tanaka M, Takigahira M, Miyazawa Y, Nakanishi Y, Kanai Y *et al.* (2008). CUB-domain-containing protein 1 regulates peritoneal dissemination of gastric scirrhous carcinoma. *Am J Pathol* **172**: 1729–1739.

Yanagihara K, Takigahira M, Tanaka H, Komatsu T, Fukumoto H, Koizumi F *et al.* (2005). Development and biological analysis of peritoneal metastasis mouse models for human scirrhous stomach cancer. *Cancer Sci* **96**: 323–332.

Yeatman TJ. (2004). A renaissance for SRC. *Nat Rev Cancer* **4**: 470–480.

Yoon HY, Lee JS, Randazzo PA. (2008). ARAP1 regulates endocytosis of EGFR. *Traffic* **9**: 2236–2252.

Supplementary Information accompanies the paper on the Oncogene website (http://www.nature.com/onc)

Engulfment of hematopoietic stem cells caused by down-regulation of CD47 is critical in the pathogenesis of hemophagocytic lymphohistiocytosis

Takuro Kuriyama,[1] Katsuto Takenaka,[1] Kentaro Kohno,[2] Takuji Yamauchi,[1] Shinya Daitoku,[1] Goichi Yoshimoto,[3] Yoshikane Kikushige,[1] Junji Kishimoto,[4] Yasunobu Abe,[5] Naoki Harada,[3] Toshihiro Miyamoto,[1] Hiromi Iwasaki,[2] Takanori Teshima,[2] and Koichi Akashi[1,2]

[1]Department of Medicine and Biosystemic Science, Kyushu University Graduate School of Medical Sciences, Fukuoka, Japan; [2]Center for Cellular and Molecular Medicine, Kyushu University Hospital, Fukuoka, Japan; [3]Department of Hematology, Kyushu Medical Center, Fukuoka, Japan; [4]Digital Medicine Initiative, Kyushu University, Fukuoka, Japan; and [5]Department of Medicine and Bioregulatory Science, Kyushu University Graduate School of Medical Sciences, Fukuoka, Japan

Hemophagocytic lymphohistiocytosis (HLH) is characterized by deregulated engulfment of hematopoietic stem cells (HSCs) by BM macrophages, which are activated presumably by systemic inflammatory hypercytokinemia. In the present study, we show that the pathogenesis of HLH involves impairment of the antiphagocytic system operated by an interaction between surface CD47 and signal regulatory protein α (SIRPA). In HLH patients, changes in expression levels and HLH-specific polymorphism of SIRPA were not found. In contrast, the expression of surface CD47 was down-regulated specifically in HSCs in association with exacerbation of HLH, but not in healthy subjects. The number of BM HSCs in HLH patients was reduced to approximately 20% of that of healthy controls and macrophages from normal donors aggressively engulfed HSCs purified from HLH patients, but not those from healthy controls in vitro. Furthermore, in response to inflammatory cytokines, normal HSCs, but not progenitors or mature blood cells, down-regulated CD47 sufficiently to be engulfed by macrophages. The expression of prophagocytic calreticulin was kept suppressed at the HSC stage in both HLH patients and healthy controls, even in the presence of inflammatory cytokines. These data suggest that the CD47-SIRPA antiphagocytic system plays a key role in the maintenance of HSCs and that its disruption by HSC-specific CD47 down-regulation might be critical for HLH development. (*Blood.* 2012;120(19):4058-4067)

Introduction

Hemophagocytic lymphohistiocytosis (HLH) is a syndrome with excessive immune activation characterized by deregulated engulfment of hematopoietic cells by macrophages in the BM. Patients with HLH display hemophagocytosis, pancytopenia, and various inflammatory symptoms, including high fever, acute liver failure, and splenomegaly.[1-4] HLH is classified into primary HLH and secondary HLH. Primary HLH, also known as familial hemophagocytic lymphohistiocytosis, shows clear familial inheritance or genetic causes, including mutations in the perforin (PRF1), MUNC13-4, syntaxin 11 (STX11), and RAB27A genes.[5-9] In primary HLH, natural killer cells and/or cytotoxic T lymphocytes fail to eliminate the targets in response to inflammatory reactions, and the resulting sustained inflammatory responses induce deregulated activation of macrophages. In secondary HLH, macrophages are activated in association with infections and malignant disorders.[4] The key pathogenic feature of HLH is hypercytokinemia including IFN-γ, TNF-α, IL-6, and M-CSF, which may activate macrophages to engulf blood cells.[3] These cytokines are produced mainly by natural killer cells and cytotoxic T lymphocytes, and might stimulate BM macrophages to engulf erythrocytes, leukocytes, platelets, and their precursors in the BM.

The question is, if hypercytokinemia causes activation of macrophages to engulf blood cells, why does such activation occur specifically in BM macrophages and induce severe hypocellularity and pancytopenia? Engulfment is triggered by the binding of specific receptors on macrophages to their ligands. Receptors on macrophages include phosphatidylserine receptors and low-density lipoprotein-related protein (LRP).[10-14] Lipopolysaccharide and calreticulin (CRT) are typical ligands for these macrophage receptors to induce a prophagocytic signal.[14,15] The phosphatidylserine-phosphatidylserine receptor system predominantly serves as a prophagocytic signal for macrophages during apoptosis.[13,16] In contrast, the CRT-LRP system also works on viable cells,[14] so there must be a mechanism to prevent inadequate engulfment of viable cells. Self-recognition to prevent phagocytosis is regulated by the CD47 and signal regulatory protein α (SIRPA) interaction, and CD47-SIRPA signaling plays an important role in preventing phagocytosis of cells.[17,18] Therefore, phagocytosis of viable cells is regulated by the balance of prophagocytic CRT-LRP and antiphagocytic CD47-SIRPA signals for macrophages, indicating that the balance of this signaling is deregulated in HLH.

CD47 is a member of the Ig superfamily that is ubiquitously expressed in hematopoietic and nonhematopoietic cells.[17,18] CD47 interacts with SIRPA through its respective IgV-like domains.[18] In contrast, SIRPA is a transmembrane protein that contains 3 Ig-like domains within the extracellular region. SIRPA is expressed in macrophages, myeloid cells, and neurons.[18-21] The cytoplasmic region of SIRPA has immunoreceptor tyrosine-based inhibitory

Submitted February 5, 2012; accepted August 26, 2012. Prepublished online as *Blood* First Edition paper, September 18, 2012; DOI 10.1182/blood-2012-02-408864.

The online version of this article contains a data supplement.

The publication costs of this article were defrayed in part by page charge payment. Therefore, and solely to indicate this fact, this article is hereby marked "advertisement" in accordance with 18 USC section 1734.

motifs.[18] Binding cell-surface CD47 with SIRPA on macrophages provokes inhibitory signals through phosphorylation of the immunoreceptor tyrosine-based inhibitory motifs of SIRPA, activating inhibitory tyrosine phosphatases such as SHP1 and SHP2.[18] This signaling inhibits myosin assembly of macrophages, thereby inhibiting phagocytosis.[18] The CD47-SIRPA self-recognition system is primarily used in RBC clearance to maintain homeostasis of the blood.[22]

Interestingly, this system also plays a critical role in engraftment of hematopoietic stem cells (HSCs) in xenotransplantation. Transplantation of the BM of CD47-deficient mice could not rescue lethally irradiated wild-type mice,[23] probably due to engulfment of CD47-deficient HSCs by BM macrophages that constitute the HSC niche.[24,25] In addition, we have reported previously that polymorphism of the SIRPA IgV domain can modulate the binding affinity of mouse SIRPA to human CD47 and plays a decisive role in xenotransplantation of human HSCs into mice; NOD, a mouse line known to have very efficient engraftment of human hematopoiesis, has a SIRPA polymorphism that can recognize human CD47, and this binding produces inhibitory signaling for mouse macrophages not to engulf human HSCs.[26]

These previous data led us to hypothesize that the BM-specific macrophage activation in HLH is caused by disruption of the CD47-SIRPA self-recognition system. In the present study, we show that in HLH, inflammatory cytokines down-regulate CD47, especially at the HSC stage, which can provoke the engulfment of HSCs by macrophages.

Methods

Patients and samples

Supplemental Table 1 (available on the *Blood* Web site; see the Supplemental Materials link at the top of the online article) summarizes the clinical characteristics of the patients. During the period from October 2005 to April 2011, 24 patients were diagnosed with HLH. The diagnosis of HLH was made according to HLH-2004 diagnostic guideline[27] and Tsuda-97.[28] The median age was 36 years (range, 16-71). Etiologies were documented in 12 patients: EBV (n = 7), CMV (n = 1), diffuse large B-cell lymphoma (n = 1), EBV^+ diffuse large B-cell lymphoma (n = 1), defective PRF1 (n = 1), and adult onset Still disease (n = 1). The median hemoglobin level was 11.1 g/dL (range, 6.2-16.2), the median platelet count was 54.8×10^9/L (range, 4-187), and the median ferritin level was 4530 ng/mL (range, 620-44 020). Prednisolone-based treatment was used in 14 patients (58%), and HSC transplantation was performed in 2 patients (8%). BM and peripheral blood samples were obtained from healthy volunteers (n = 50) and HLH patients (n = 24). Cord blood samples from full-term deliveries and normal BM samples from normal volunteers were obtained based on informed consent (provided by Kyushu Block Red Cross Blood Center, Japan Red Cross Society). Informed consent was received for all donors in accordance with the Declaration of Helsinki. The institutional review board of Kyushu University Hospital approved all experiments in this study.

Cell lines

A human acute promyelocytic leukemia cell line, NB4, which retains t(15;17), was obtained from the German Collection of Microorganisms and Cell Cultures (DSMZ). NB4 cells were cultured in RPMI 1640 medium (Wako) containing 10% FBS (ICN).

Sequence alignment of the human SIRPA IgV domains

Genomic DNA was extracted by using QIAamp DNA Blood Mini Kit (QIAGEN). The cording region of the SIRPA IgV domain was amplified by PCR. Genomic DNA was used as a PCR template in the following conditions: 10 minutes at 94°C, 30 cycles of 1 minute at 94°C, 1 minute at 60°C, 1 minute at 72°C, and 16 minutes at 72°C. PCR and sequencing primers were as follows: forward primer 5′-GCCTGCTTC-TGGTGTGCATCCAGTC-3′ reverse primer 5′-GAGTTACTGTC-ACAAACCAGAGGC-3′. PCR products were cloned to the PCR 2.1-TOPO vector (Invitrogen) and 10-25 clones were sequenced for every sample.

Abs, cell staining, and sorting

For analysis of cell-surface expression of SIRPA, we used SIRPA mAb (MBL International) and FITC-conjugated antimouse IgG (Beckman Coulter). For analysis of cell-surface expression of CD47, we used PE-conjugated anti-CD47 (BD Pharmingen). For sorting and analysis of $CD34^+CD38^-$ and $CD34^+CD38^+$ cells, cells were stained with FITC-conjugated anti-CD34 (BD Pharmingen), PE-conjugated anti-CRT (Enzo Life Sciences), peridinin chlorophyll A protein-cy5.5–conjugated anti-CD47 (BD Pharmingen), and allophycocyanin-conjugated anti-CD38 (BD Pharmingen). For some experiments, cells were stained with allophycocyanin-conjugated anti-CD34, PE-conjugated anti-CD47, and PE-Cy7 conjugated anti-CD38 (all BD Pharmingen). Before sorting and analysis, lineage cells in cord blood cells were depleted using a lineage cell depletion kit (Miltenyi Biotec). $CD34^+CD38^-$ and $CD34^+CD38^+$ cells were purified on a FACSAria cell sorter (BD Biosciences).

The analysis procedures of $CD34^+CD38^+$ progenitor populations were described previously.[29,30] BM mononuclear cells were first stained with PE-Cy5–conjugated lineage Abs, including anti-CD3, anti-CD4, anti-CD8, anti-CD10, anti-CD19, anti-CD20, anti-CD14, anti-CD56, and glycophorin A (BD Pharmingen). Subsequently, cells were stained with FITC-conjugated anti-CD34 (BD Pharmingen), PE-conjugated anti-CD47 (BD Pharmingen), PE-Cy7–conjugated anti-CD123 (eBiosciences), and Pacific Blue–conjugated anti-CD45RA (Beckman Coulter) Abs. HSCs, common myeloid progenitors, granulocyte/macrophage progenitors, and megakaryocyte/erythrocyte progenitors were isolated as $Lin^-CD34^+CD38^-$, $Lin^-CD34^+CD38^+CD123^+CD45RA^-$, $Lin^-CD34^+CD38^+CD123^+CD45RA^+$, and $Lin^-CD34^+CD38^+CD123^-CD45RA^-$ populations. The cells were analyzed and sorted with a FACSCalibur flow cytometer and a FACSAria 2 cell sorter (both BD Biosciences). The mean fluorescent intensity of CD47 and CRT was normalized and shown as a ratio to PBMCs from healthy donors.

Preparation of human macrophages from peripheral blood

Monocytes were purified from PBMCs by positive selection using MACS CD14 Micro Beads (Miltenyi Biotec). These cells were incubated with X-VIVO10 (Lonza) containing 2% AB serum and 100 ng/mL of M-CSF (R&D Systems) for more than 96 hours to obtain macrophages.[31,32]

In vitro phagocytosis assays for target cells

Peripheral blood–derived macrophages were prepared and incubated at 1.0×10^4 cells in 200 μL of RPMI 1640 medium in Falcon culture tubes (2058; BD Biosciences), and then $1.0\text{-}5.0 \times 10^4$ target cells were added to the tubes and incubated at 37°C for 2 hours. Before the addition of target cells to macrophage-containing tubes, cells were opsonized with CD34 Ab (sc-19621; Santa Cruz Biotechnology) for $CD34^+CD38^-$ cells and $CD34^+CD38^+$ cells isolated from normal and HLH BM by FACS sorting; CD13 Ab (sc-51522; Santa Cruz Biotechnolgoy) and CD33 Ab (sc-19660; Santa Cruz Biotechnology) for NB4 cells; CD45 Ab (555480; BD Pharmingen) for lymphocytes; and neutrophils and glycophorin A Ab for RBCs (555569; BD Pharmingen). For activation of macrophages, cells were incubated with IFN-γ (100 ng/mL; R&D Systems) for 24 hours and with lipopolysaccharide (0.3 μg/μL) for 1 hour, and then harvested and washed 3 times with PBS before the addition of target cells. After coincubation with macrophages and target cells, they were mounted on cytospin preparations, and 1000 macrophages were tested to enumerate engulfing ones by a blinded observer. We calculated the phagocytic index using the following formula: phagocytosis index = phagocytic macrophages/number of macrophages.[33]

Inhibition of CD47 expression by siRNA

To investigate the effect on phagocytosis according to the expression level of CD47, CD47 expression of NB4 cells and CD34$^+$ cord blood cells was down-regulated using siRNA. CD47 siRNA primers used were as follows: siRNA1, UAUACACGCCGCAAUACAGAGACUC and GAGUCUCUGUAUUGCGGCGUGUAUA; siRNA2, UAGAAGUCACAAUUAAACCAAGGCC and GGCCUUGGUUUAAUUGUGACUUCUA. The Nucleofector kit V and Human CD34 Cell Nucleofector kit (both Amaxa) were used to transfect siRNA and transfected NB4 cells, and lineage-depleted cord blood cells were incubated for 48 and 24 hours, respectively. NB4 cells and CD34$^+$CD38$^-$ cells were then sorted depending on CD47 expression using the FACSAria 2 cell sorter (BD Biosciences), and these cells were used for in vitro phagocytic assays to determine the phagocytic index.

Quantitative RT-PCR

Total RNA was extracted from normal and HLH BM. Reverse transcription was performed using a high-capacity cDNA reverse transcription kit (Applied Biosystems) according to the manufacturer's instructions. CD47 and control gene 18srRNA primers were obtained from Applied Biosystems. Amplification, detection, and quantification were performed with the TaqMan ABI Prism 7000 sequence detection system (Applied Biosystems). Data were calculated by the relative quantitation method (ΔΔCt) compared with 18srRNA as an internal control.

Measurement of cytokines by ELISA

Cytokines, including IFN-γ, TNF-α, IL-6, and M-CSF, from HLH and normal blood serum were measured with ELISA. IFN-γ was measured with the IFN-γ Quantikine ELISA kit (DIF50; R&D Systems), TNF-α was measured with the TNF-α Quantikine HS ELISA kit (HSTA00D; R&D Systems), IL-6 was measured with the IL-6 Quantikine ELISA kit (D6050; R&D Systems), and M-CSF was measured with the M-CSF Quantikine ELISA kit (DMC00B; R&D Systems).

In vitro treatment of normal HSCs with inflammatory cytokines

To evaluated the effects of inflammatory cytokines on the expression level of CD47, lineage-depleted cord blood cells were purified by negative selection using the MACS lineage cell depletion kit (Miltenyi Biotec) and cultured in 24-well dish (3047; BD Biosciences) with 300 μL of X-VIVO10 supplemented with 10% FBS and cytokines as follows: SCF (50 ng/mL; R&D Systems), M-CSF (750 pg/mL; R&D Systems), IL-6 (200 pg/mL; R&D Systems), TNF-α (20 pg/mL; R&D Systems), and IFN-γ (250 pg/mL; R&D Systems). After 24 hours of culture, CD34$^+$CD38$^-$ and CD34$^+$CD38$^+$ cells were sorted with the FACSAria 2 cell sorter (BD Biosciences), and these cells were used to determine the phagocytic index.

Statistical analysis

Statistical analysis was performed using jmp Version 9 software (SAS Institute). CD47 expression on CD34$^+$CD38$^-$ cells, CD34$^+$CD38$^+$ cells, and bulk among the groups were compared with the Dunnett test. For siRNA experiments using NB4 cells and CD34$^+$CD38$^-$ cells, phagocytic index was compared with a conventional t test. For phagocytic assays using CD34$^+$CD38$^-$ cells from cord blood cells that had been cultured with inflammatory cytokines, P values were obtained by ANCOVA. $P < .05$ was considered statistically significant.

Results

Changes in expression levels of SIRPA or SIRPA mutations do not occur in HLH patients

Several variants of the IgV domain in SIRPA (exon3 of SIRPA), where the CD47-binding site is located, have been reported in human.[26,34] We first tested the possibility that the SIRPA polymorphism may influence the development of HLH. We examined the sequence alignment of SIRPA IgV domain of 50 Japanese healthy donors. Although many polymorphisms have been reported previously in the SIRPA IgV domain,[26] we identified 2 variants (variants 1 and 2) in the present study (Figure 1A). There are 13 amino acid differences between these 2 variants as we have described,[26] and

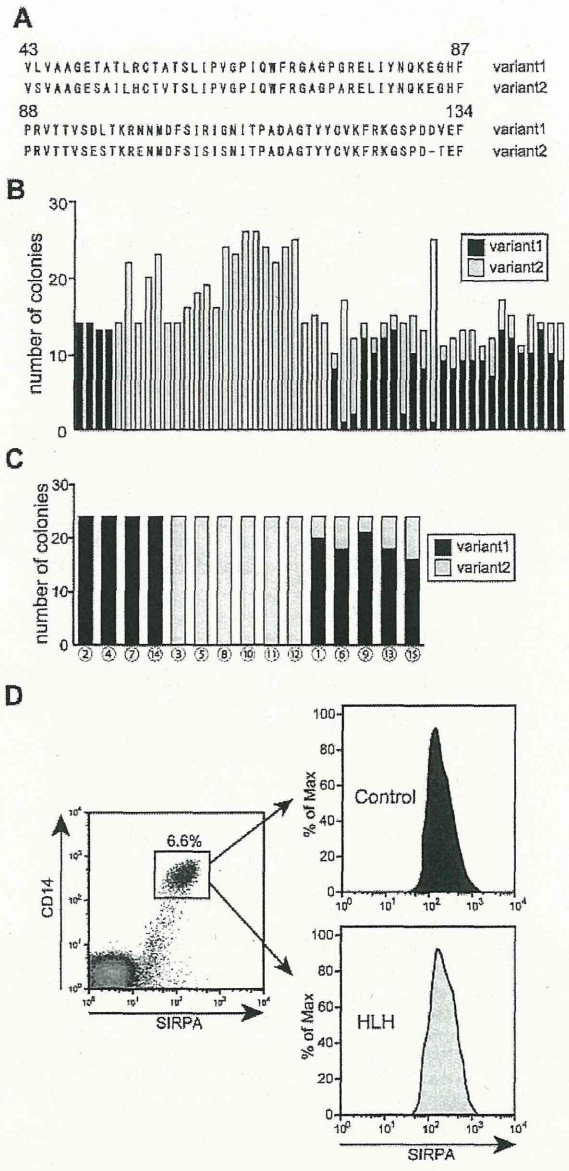

Figure 1. SIRPA mutation or changes of its expression level is not involved in pathogenesis of HLH. (A) Sequence alignment of SIRPA IgV domains (exon 3 of SIRPA) identified by sequence analysis from genomic DNA of 50 healthy donors. Two variants, which we have described previously,[20] were identified in the present study. There are 13 amino acid differences between these 2 variants. (B) Distribution of genotype of SIRPA IgV domains in 50 healthy donors. PCR products were cloned to pCR 2.1-TOPO vector and 10-25 clones were sequenced for every sample: 24 were heterozygous for variants 1 and 2, 4 were homozygous for variant 1, and 22 were homozygous for variant 2. (C) Distribution of genotype of SIRPA IgV domains in 15 HLH patients (unique patient number [UPN] 1-15); 4 (UPN 2, 4, 7, and 14) were heterozygous of variants 1 and 2, 6 (UPN 3, 5, 8, 10, 11, and 12) were homozygous for variant 1, and 5 (UPN 1, 6, 9, 13, and 15) were homozygous for variant 2. There were no other variants or changes of SIRPA IgV domain in HLH patients. (D) Representative expression of surface SIRPA on CD14$^+$ cells of control and HLH patients on FACS. There was no significant difference in the expression level of SIRPA in CD14$^+$ monocytes between HLH and normal BM: The mean ± SD of CD47 fluorescence intensity was 116 ± 1.7 and 118 ± 9.6 in healthy controls (n = 5) and HLH patients (n = 5), respectively (P = .88).

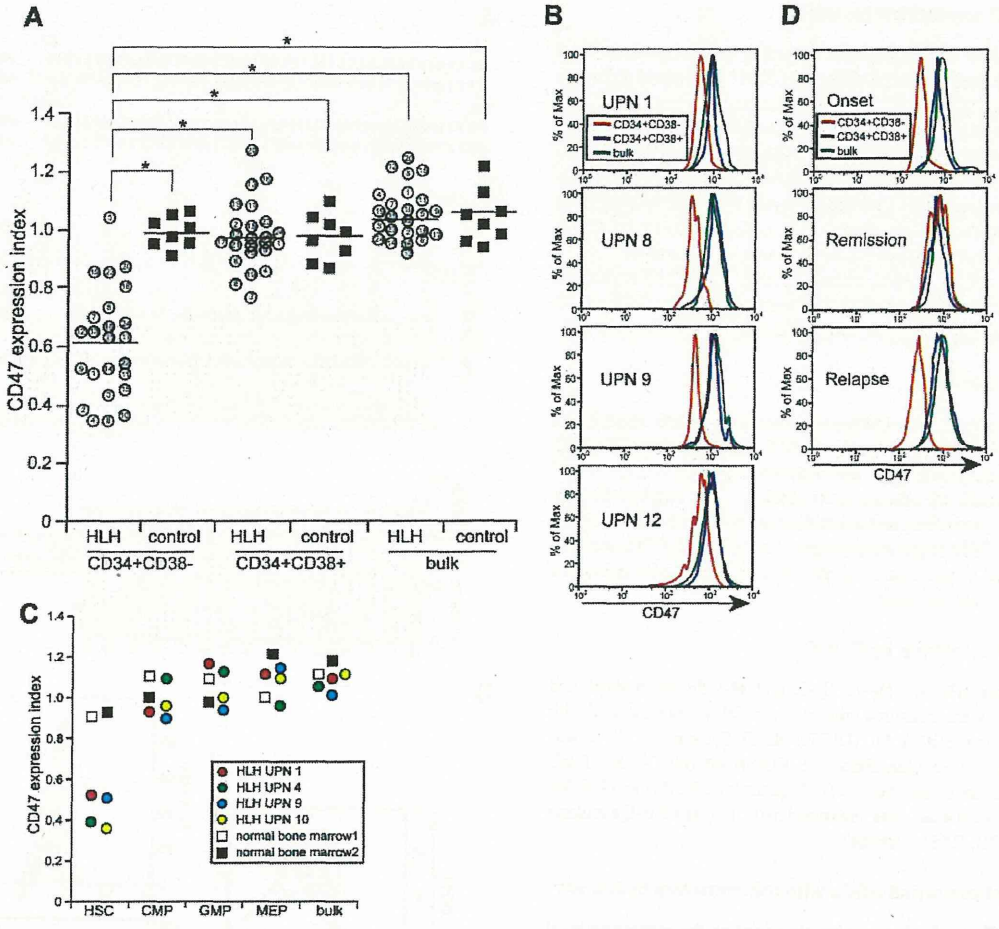

Figure 2. CD47 expression is down-regulated specifically in the CD34$^+$CD38$^-$ HSC fraction in HLH patients, reflecting the disease activity. (A) CD47 expression of CD34$^+$CD38$^-$ cells, CD34$^+$CD38$^+$ cells and unfractionated BM cells in HLH patients and healthy controls. The number in each open circle corresponds to the unique patient number (UPN) of patients (supplemental Table 1). The horizontal bars in each group show mean values of the group. The level of CD47 on CD34$^+$CD38$^-$ cells was significantly decreased compared with that on CD34$^+$CD38$^+$ cells and more mature cells. The CD47 expression index represents the relative surface CD47 level (median CD47 levels of analyzed cells/those in normal blood mononuclear cells). (B) Histograms of CD47 expression of BM cells in 4 representative HLH patients (UPN 1, 8, 9, and 12). (C) CD47 expression of CD34$^+$CD38$^-$ HSC-enriched fraction and of each progenitor cell fraction in HLH patients (UPN 1, 4, 9, and 10) and healthy controls. All progenitor populations expressed equivalent levels of CD47, and CD47 expression was down-regulated only in HSC fraction. (D) Change of CD47 expression in UPN 10 during multiple episodes of HLH. Down-regulation of CD47 repeatedly occurred at exacerbation of HLH.

their binding capacity to CD47 was equal.[34] Twenty-four of 50 healthy donors were heterozygous for variants 1 and 2, 4 were homozygous for variant 1, and 22 were homozygous for variant 2 (Figure 1B). Similarly, we examined sequence alignment of SIRPA IgV domain of 15 HLH patients, in whom we identified variant 1 and variant 2 SIRPA IgV-encoding alleles, but no other variants or changes in the allele burden of variants 1 and 2 (Figure 1C). Furthermore, the expression level of SIRPA on the cell surface did not differ among HLH and normal BM cells (data not shown) and CD14$^+$ cells (Figure 1D). These data suggest that alterations in SIRPA or its expression are not involved in the pathogenesis of HLH.

CD47 is down-regulated in the CD34$^+$CD38$^-$ HSCs from HLH patients

We also evaluated the expression level of CD47 in the BM of HLH patients. As shown in Figure 2A, the control normal BM cells ubiquitously express CD47. Its expression levels were always high in the CD34$^+$CD38$^-$ fraction that concentrates HSCs,[35] in the CD34$^+$CD38$^+$ progenitor fraction, and in unfractionated cells that mainly contained mature cells. In the HLH BM, CD47 expression is down-regulated specifically in the CD34$^+$CD38$^-$ HSC fraction compared with those in the progenitor and mature cell fraction by approximately 2-fold at the expression level (Figure 2A-B). To determine more precisely the expression of CD47 in progenitor fractions, we subfractionated CD34$^+$CD38$^+$ progenitors into common myeloid progenitor, granulocyte/macrophage progenitor, and megakaryocyte/erythrocyte progenitor populations.[29] These progenitors had equivalent levels of CD47 (Figure 2C and supplemental Figure 1). The down-regulation of CD47 occurs in conjunction with the deterioration of HLH. Patient number 10, who suffered from adult onset primary HLH due to defective PRF1,[36] had repeated episodes of HLH. The follow-up of this patient revealed that the expression levels of CD47 in HSCs normalized in remission, but its down-regulation occurred again at exacerbation of the disorder (Figure 2D). These data strongly suggest that the HSC stage-specific down-regulation of CD47 plays a critical role in HLH development.